Scanning Electrochemical Microscopy: Measurement of the Current Density at Microscopic Redox-Active Sites on Titanium

Solomon B. Basame and Henry S. White*

Department of Chemistry, University of Utah, Salt Lake City, Utah 84112

Received: May 1, 1998; In Final Form: June 26, 1998

Absolute values of the current density at microscopic electroactive sites on polycrystalline Ti electrodes have been measured with a scanning electrochemical microscope (SECM). The active sites on the oxide-film-coated Ti electrode have radii ranging from 3.3 to 28.6 μm and are randomly distributed at a surface density of ~180 sites/cm^2. Localized current densities as large as 0.14 A/cm^2 are observed for the oxidation of Br^- in aqueous solution, approximately 4 orders of magnitude larger than the average current density based on the geometrical area of the electrode. Quantitative analysis of large-area SECM images demonstrates that at least ~65% of the total current during Br^- oxidation is associated with sites that occupy a minuscule fraction (0.01−0.1%) of the total exposed electrode area. The SECM data also suggest that the rate of Br^- oxidation approaches the diffusion-limited value at sites having radii less than ~10 μm; a precipitous decrease in the electron-transfer rate is observed at electroactive sites of slightly larger dimensions.

Introduction

We wish to report the measurement of the current density associated with electron-transfer reactions at randomly distributed electroactive sites at the surface of Ti electrodes. Recent reports from our laboratory[1−3] and elsewhere[4] have described highly localized electrochemical activity at Ti surfaces on which a native or anodically grown semiconducting oxide film has been deposited; hereafter we refer to the oxide-covered metal electrode as Ti/TiO_2. Visualization of the electroactive sites, having dimensions of the order of 10 μm, is made possible by scanning electrochemical microscopy (SECM), a scanned-probed method in which a microelectrode, poised at constant potential, is rastered across the substrate and used to amperometrically detect electrochemically active species generated at the substrate surface.[5,6] Spatially localized activity is observed on Ti/TiO_2 for redox reactions that occur at potentials positive of the conduction band edge (E_c) of TiO_2, e.g., the oxidation of $Fe(CN)_6^{4-}$. These reactions occur at electroactive sites that have metal-like properties, i.e., they are electrochemically active at potentials within the band gap region of the oxide where no electronic states are expected to be available for electron transfer. Conversely, SECM images also demonstrate that the reduction of a redox species at potentials negative of E_c is spatially uniform across the surface,[3] consistent with the accumulation of electrons at the surface of the n-type oxide semiconductor at negative potentials.[7] These results, as well as the SECM investigations by Horrocks et al. of heterogeneous electron transfer on Si and metal dichalcogenide electrodes,[8] demonstrate the unique capability of SECM for mapping spatially localized and potential-dependent reactions on semiconducting surfaces.

While our previous SECM studies provide a qualitative understanding of the behavior of the electroactive sites on Ti/TiO_2, a quantitative investigation of electron-transfer kinetics at these sites has not been reported. Of particular interest is the determination of the fraction of the total electrode current that is associated with the microscopic sites. This is a challenging analytical problem due to the small size, random distribution, and extremely low number density of active sites. In addition, as shown below, the redox-active sites display widely varying electron-transfer kinetic properties. The problem requires measurement of the current density (or its equivalent, the electron-transfer rate constant) and the area of each electroactive site on the electrode surface. To our knowledge, a quantitative electrochemical analysis of this type has never been performed.

Bard et al. have developed SECM methodology for analysis of heterogeneous electron-transfer kinetics at microdisk electrodes having dimensions comparable to the sites present on the Ti/TiO_2 surface.[9] However, their method is not readily extended to quantifying the current distribution across a surface for a redox reaction that occurs at many discrete sites. In the present report, the current densities at individual electroactive sites on Ti/TiO_2 electrodes have been measured using SECM methodology recently developed for the analysis of molecular transport in porous membranes.[10] As discussed in detail below, the SECM analysis allows quantitative evaluation of the absolute current density of individual redox-active sites as well as the dimensions of the sites. The methodology reported here is generally applicable to any heterogeneous surface containing an arbitrary number of randomly positioned sites, each of different size and/or displaying different electron-transfer kinetics. SECM analysis of every electroactive redox site on several large-area Ti/TiO_2 electrodes has been performed, and the results used to determine the fraction of the total current that is associated with the microscopic sites. We show that a small number of microscopic electroactive sites, occupying a remarkably small percentage of the total exposed area, can dominate the overall electrochemical behavior of the Ti/TiO_2 electrode.

Experimental Section

Chemicals. Potassium ferrocyanide, potassium bromide, sodium chloride, and sulfuric acid (all from Mallinckrodt) were used as received. All aqueous solutions were prepared using 18 MΩ cm water obtained from a Barnstead E-pure purification system.

10.1021/jp982088x CCC: $15.00
Published on Web 08/19/1998

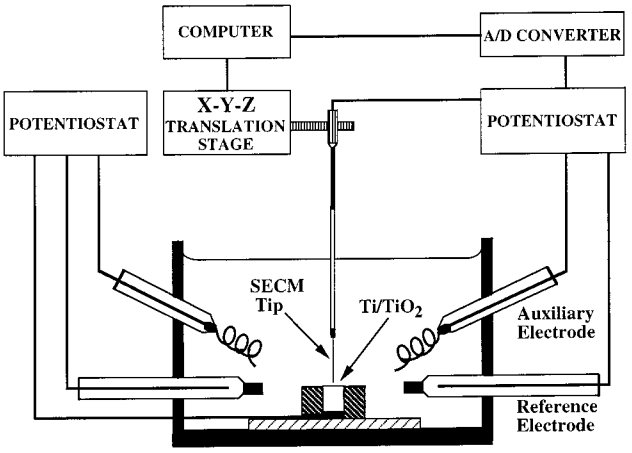

Figure 1. (a) Schematic diagram of the SECM.

Preparation of Electrodes. Au and Pt microdisk electrodes were fabricated using 12.5- and 25-μm-radius Pt wires and 6-μm-radius Au wire (Johnson Matthey). A ~1.5-cm-long wire was sealed in a glass tube using an acetylene flame. A 90° bend was made in the glass tube to facilitate SECM experiments in which the microdisk electrode is facing upward. The sealed end was carefully sanded to expose a disk surface. A Cu wire was attached to the Au or Pt wire with Ag epoxy. Prior to each experiment, the Au or Pt disk electrode was polished with 0.3-μm alumina (Johnson Matthey) and thoroughly rinsed with distilled water. The radius of the exposed disk, a, was determined before each experiment by recording the steady-state limiting current, i_{lim}, for the oxidation of $Fe(CN)_6^{4-}$. The electrode radius is related to i_{lim} by eq 1, where C^* is the

$$i_{lim} = 4nFDC^*a \qquad (1)$$

concentration of redox species in the bulk solution, D is the diffusivity of $Fe(CN)_6^{4-}$ (0.65×10^{-5} cm^2/s), F is Faraday's constant, and n is the number of electrons transferred per molecule.

The Ti electrode was prepared from a 3.175-mm-diameter Ti rod (Johnson Matthey). A Cu lead was attached to a 0.5-cm-long piece of the Ti rod using conductive Ag epoxy. The rod was insulated by placing it in a 1-cm-diameter PVC tube containing 86% (by weight) Shell Epon Resin 825 (Miller-Stephenson Chemical) and 14% 1,3-phenylenediamine (Aldrich Chemical) at 100 °C. After being cured overnight at 65 °C, the PVC tube was removed, leaving a hardened polymer cast around the Ti rod. The end of the rod was ground flat on silicon carbide paper to expose the 3.175-mm-diameter Ti disk-shaped electrode. The electrode assembly was mounted on a glass slide that served as a sample holder in the SECM cell. Prior to each experiment, the Ti disk was gently polished, in one direction, on a dry silicon carbide 1200 grit sanding paper (Metlab Corp.) and thoroughly rinsed with water.

Scanning Electrochemical Microscopy. Figure 1 shows a schematic diagram of the essential components of the scanning electrochemical microscope (SECM). The substrate potential (E_s) and the SECM tip potential (E_t) are independently controlled in two separate potentiostatic circuits. In the studies reported here, E_s is set at a value to either oxidize or reduce a reactant species that is present in the bulk of the solution, while E_t is held at a potential to detect the products that are electrogenerated at the substrate. This mode of SECM operation is referred to by Bard and co-workers as the substrate generation/tip collection mode (SG/TC mode).[11]

A detailed description of the in-house-built SECM has been previously reported by Scott et al.[12,13] A C-fiber SECM tip, Pt wire auxiliary electrodes, and Ag/AgCl reference electrodes are used in these studies. To acquire an SECM image, the C-fiber SECM tip is scanned across the sample surface at a fixed height and the tip current is recorded as a function of its spatial position. Data are collected and plotted in real time and stored as ASCII files. Axes movement and data acquisition are controlled with a PC using several virtual instrument subroutines written in LabView (National Instruments).

The SECM probe tip is an ~4-μm-radius C fiber (Johnson Matthey, Inc.) that was partially sealed in a glass microcapillary (Drummond Scientific, Inc.). Ag epoxy was used to create an electrical contact to the end of the C fiber that is encased in the glass capillary. The exposed surface of the C fiber was insulated by electrochemical deposition of an ~3-μm-thick layer of polyphenylene oxide.[14] The insulating layer was deposited by biasing the carbon fiber at 4 V for 20 min in a 40:60 water/methanol solution containing 0.25 M 2-allylphenol, 0.2 M 2-butoxyethanol, and 0.4 M ammonium hydroxide. Following deposition, the electrode was rinsed with the solvent mixture and cured at 120 °C for 1 h. The voltammetric response of the coated C fiber was recorded in a solution containing 10 mM $K_4Fe(CN)_6$ and 0.1 M NaCl in order to check the quality of the insulating film. No faradaic response was measured at the C fiber, indicating successful insulation. The end of the C fiber was then cut using a razor blade to expose a C microdisk electrode. The voltammetric response of this electrode in the 10 mM $K_4Fe(CN)_6$ solution displayed a sigmoidal waveshape, corresponding to the diffusion-limited oxidation of $Fe(CN)_6^{4-}$ at the exposed C surface. The radius of each C electrode was determined from the voltammetric limiting current using eq 1, as described above.

Following the assembly of the components of the SECM cell, the SECM tip is slowly lowered onto the substrate surface (at open circuit) until a gentle contact is made. Using a video microscope with a zoom lens for viewing, the tip is then retracted in the z direction in increments of 0.2 μm until it is observed to travel freely in the $x-y$ plane. The tip is retracted by an additional 2−5 μm in order to prevent contact with the surface during imaging of large areas. The tip is scanned during imaging at a velocity between 2 and 10 μm/s.

Results and Discussion

The results are presented in the following order. In section I, a qualitative description of SECM images of Ti/TiO_2 in aqueous Br^- solutions is presented, along with details of the imaging mechanism. Large-area SECM imaging and factors that influence recognition of microscopic redox-active sites on Ti/TiO_2 are presented in section II. The methodology used for quantifying electron-transfer kinetics at a single electroactive site is developed in section III and applied in section IV to the kinetic analysis of elecroactive sites on Ti/TiO_2. The SECM-based analysis described in section III is applicable to any heterogeneous surface and not limited to the current application. Finally, in section V, the analysis of multiple electroactive sites on several large-area electrodes is presented. These latter results are used to quantify the distribution of size and kinetic activity of the electroactive sites and to determine the fraction of the total electrode current associated with these sites.

I. General Description of SECM Images of Ti/TiO_2. Figure 2a shows a 300×300 μm^2 SECM image of the Ti/TiO_2 electrode. This image was obtained in an aqueous solution containing 10 mM H_2SO_4 as the supporting electrolyte and 50

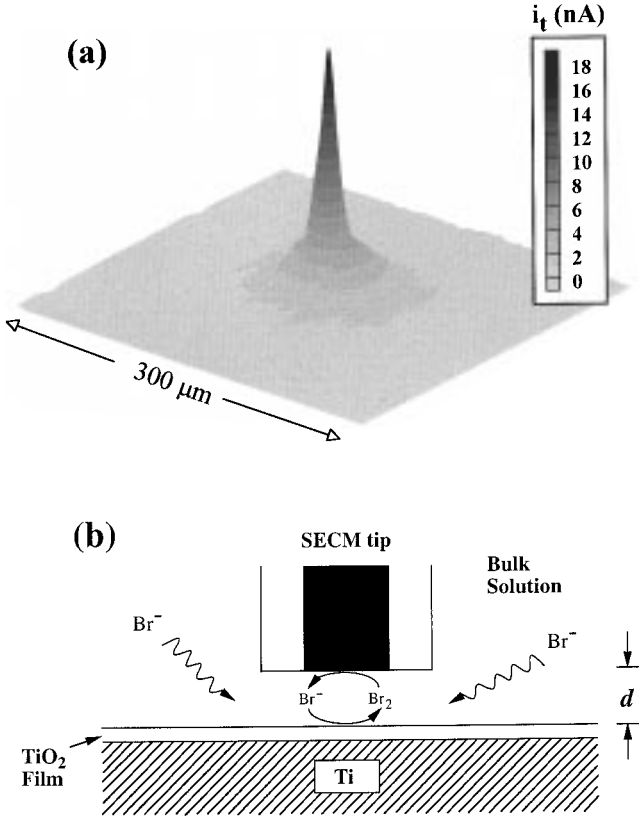

Figure 2. (a) A 300 × 300 μm SECM image of an electroactive site in a solution containing 50 mM KBr and 10 mM H_2SO_4. The potential of the Ti/TiO_2 electrode (E_s) was held at 1.5 V to oxidize Br^-. The potential of the SECM tip (E_t) was held at 0.0 V, sufficiently negative to reduce Br_2 at the mass-transport limited rate. The SECM tip was scanned at a height, d, of ~5 μm above the Ti/TiO_2 electrode. The image was recorded after the current at the Ti/TiO_2 electrode had decayed to a steady-state value. (b) Schematic drawing depicting the SECM tip positioned above an oxide-covered Ti electrode. The tip radius and tip-to-Ti electrode separation are drawn approximately to scale. The TiO_2 film (~65 Å) is much thinner than drawn.

mM KBr as the redox-active species employed in the imaging mechanism. The peak at the center of the image corresponds to a single electroactive site on the Ti/TiO_2 surface where Br^- is oxidized to Br_2. To acquire this image, the Ti/TiO_2 electrode was biased at 1.5 V vs Ag/AgCl, a potential sufficiently positive of the standard redox potential of the Br^-/Br_2 couple ($E°_{Br^-/Br_2}$ = 0.89 V vs Ag/AgCl) to cause the oxidation of Br^-. The SECM tip potential, E_t, is held at 0.0 V in order to detect, by electrochemical reduction, Br_2 as it diffuses away from the Ti/TiO_2 surface. The schematic diagram at the bottom of Figure 2 depicts the reactions that are operative during imaging. No peaks are observed in SECM images of Ti/TiO_2 that are obtained in solutions containing H_2SO_4 only.

Figure 3 shows the voltammetric response (initial scan and steady-state behavior) of the Ti/TiO_2 disk electrode in the 10 mM H_2SO_4/50 mM KBr solution and in a blank solution containing only 10 mM H_2SO_4. The initial voltammetric response (upper curves) in either solution displays a large flat background current due to oxide growth. A peak-shaped wave is observed at ~1.75 V in the solution containing 50 mM Br^-, corresponding to Br^- oxidation. The voltammetric current on the second and subsequent scans (lower curves) is reduced by about a factor of 100 due to thickening of the oxide film, which tends to passivate the surface against electrochemical reactions. Using previously reported ellipsometric data, we estimate the oxide film to be ca. 65 Å thick following a potential excursion

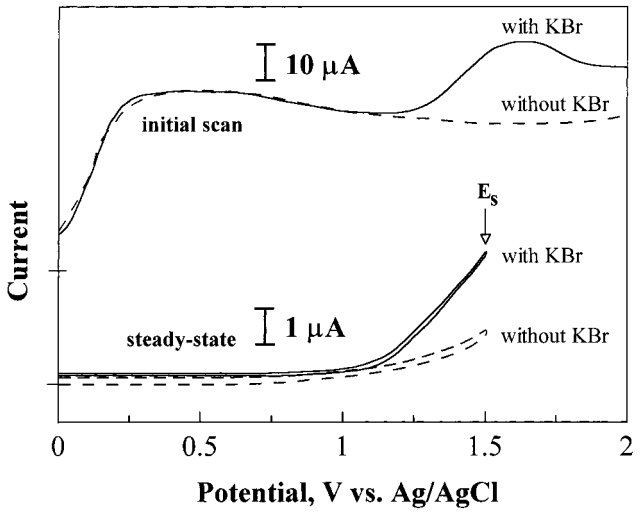

Figure 3. The initial-scan and steady-state voltammetric responses of a Ti/TiO_2 electrode in a 50 mM KBr/10 mM H_2SO_4 solution (solid lines) and in a blank solution containing only supporting electrolyte (10 mM H_2SO_4, dashed lines); scan rate = 20 mV/s. The substrate (E_s) potential during SECM imaging is indicated on the steady-state voltammetric curve.

to 2 V on the first scan.[15] Although the current is greatly reduced due to the increased kinetic overpotential, the oxidation of Br^- at the Ti/TiO_2 electrode is still clearly observed in the steady-state voltammetric response, Figure 3, as indicated by the increase in current beginning at about ~1.0 V.

During SECM imaging experiments, the Ti/TiO_2 substrate potential, E_s, is held at 1.5 V to oxidize Br^- at a steady rate (E_s is indicated on the steady-state voltammetric curve in Figure 3). The steady-state current at E_s is referred to as the *total* current, i_{tot}, since i_{tot} comprises the sum of the current at the individual electroactive sites plus any residual low-level current on the remaining oxide-covered surface. One goal of the SECM experiments reported herein is to quantify the fraction of i_{tot} that is associated with the microscopic sites. Although the voltammetric response of different Ti/TiO_2 electrodes is qualitatively similar to that shown in Figure 3, the magnitude of i_{tot} varies by a factor of 2 from one electrode to another, despite significant effort to obtain better reproducibility. This variation is believed to be related to polishing of the electrode between experiments; the use of coarser polishing papers and powders results in a larger i_{tot}.

The steady-state voltammetric response of a SECM tip positioned directly above an electroactive site is shown in Figure 4a. The tip response is characterized by both cathodic and anodic waves: the cathodic wave corresponds to reduction of Br_2 that is generated at the Ti/TiO_2 surface and diffuses back to the tip (as depicted in Figure 2b); the anodic wave corresponds to oxidation of Br^- that is present in the bulk solution. The anodic and cathodic waves are centered at $E°_{Br^-/Br_2}$ consistent with the electrogeneration of Br_2 at the electroactive site on Ti/TiO_2. The magnitudes of both waves are a function of the separation distance, d, between the tip and substrate, in agreement with theoretical predictions and previous experimental studies of positive and negative feedback phenomena in SECM.[9,16,17] A brief explanation of the distance dependence is given here. When the tip potential, E_t, is negative of $E°_{Br^-/Br_2}$, the fluxes of Br^- and Br_2, which are transported in a steady-state cycle between the tip and substrate (see Figure 2b), increase as d is decreased, resulting in a larger cathodic voltammetric current at the SECM tip (positive feedback). Conversely, when $E_t > E°_{Br^-/Br_2}$, a decrease in d results in a decrease in the anodic

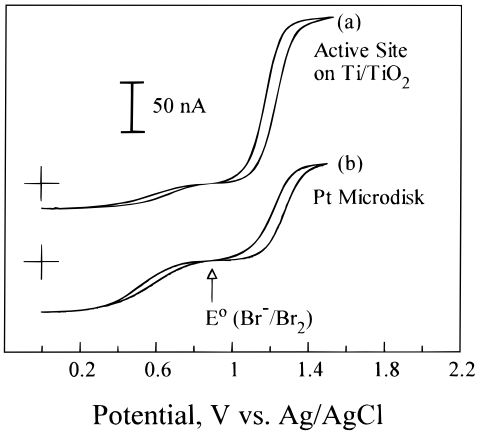

Figure 4. Cyclic voltammetric response of a SECM tip: (a) over an active site on Ti/TiO_2 in a 50 mM KBr/10 mM H_2SO_4 solution (E_s = 1.5 V, $d \approx 10$ μm) and (b) over a Pt disk electrode in 10 mM KBr/10 mM H_2SO_4 solution (E_s = 1.2 V, $d \approx 20$ μm).

current, a result of two factors: (1) the substrate blocking the transport of the Br^- from the bulk solution to the SECM tip (negative feedback) and (2) the consumption of Br^- at the active site.

As shown in Figure 4b, an essentially identical voltammetric response is observed when the SECM tip is centered above a 12.5-μm-radius Pt microdisk, the latter poised at a potential to effect the oxidation of Br^- at the diffusion-limited rate. The Pt microdisk electrode is intended to mimic a single active site on the Ti/TiO_2 surface. The similarity in the voltammetric response of the SECM tip above Pt and Ti/TiO_2 indicates that Br_2 is indeed being generated at the active sites on Ti/TiO_2.

II. Large-Area SECM Analysis. Entire surfaces of several Ti/TiO_2 electrodes (0.079 cm^2 area) were imaged by SECM in order to determine the number density of sites and the positions of every electroactive site. Large-area SECM imaging was performed as follows: with the substrate and tip potentials set at appropriate values for data acquisition, the tip is positioned close to the substrate surface ($\sim$4 μm) and scanned slowly (10 μm/s) in the *x*-direction. A video recorder with zoom lens assembly is used to observe the position of the SECM tip on the surface. Upon reaching the edge of the Ti disk, the scan is halted and the tip stepped 10 μm in the *y*-direction. The tip is then scanned in the opposite direction of the initial *x*-scan and the routine continued until the entire Ti/TiO_2 disk surface is mapped.

Figure 5 shows the cross-sectional profiles of SECM images obtained above 12 sites that were identified on the surface of one Ti/TiO_2 electrode. The profiles of tip current versus position are arranged in Figure 5, from top to bottom, in order of decreasing current. The current above individual sites varies significantly from one site to the next, ranging from $\sim$1 to 20 nA. This variability is due to differences in the size and electron-transfer kinetics of individual sites, an issue that is addressed below in more detail.

The entire surfaces of five Ti/TiO_2 electrodes were imaged in Br^- solutions. The number of sites counted on each electrode ranged from 12 to 16, yielding an average number density of $\sim$180 sites/cm^2. This value is a factor of 6 times larger than the corresponding value previously determined using *unpolished* Ti foil electrodes[1−3] instead of the polished Ti disks employed here. The larger number of sites on the Ti disks is most likely due to the polishing of these electrodes, resulting in a less uniform oxide film thickness.

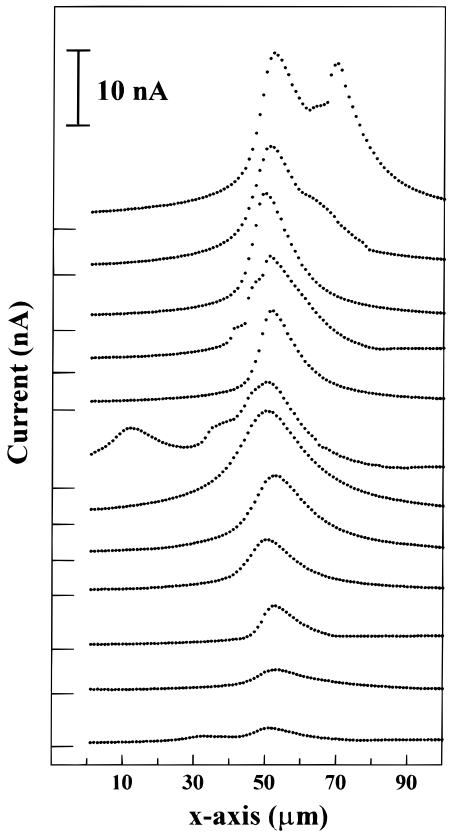

Figure 5. SECM profiles of the current distribution over 12 different active sites on a Ti/TiO_2 surface in a solution containing 50 mM KBr and 10 mM H_2SO_4 (E_s = 1.5 V, E_t = 0.0 V, and d = 5 μm for each scan).

It is entirely possible, and even probable, that there are electroactive sites on the surface that are not detected in the SECM analysis. Our detection limit in these experiments corresponds to SECM tip currents of about 0.5 nA. Sites that are either very small or at which the electron-transfer rate is low may go undetected. However, we show in the following sections that the total current, i_{tot}, associated with Br^- oxidation can be nearly accounted for by redox reactions occurring at those sites that *are observable*. Thus, although it is likely that some electroactive sites do not generate enough Br_2 to be observed in the SECM image, the contribution of these sites to the total current, i_{tot}, appears to be relatively small.

Figure 5 shows that some electroactive sites appear as double peaks. The occurrence of such multiple peaks is rare; the majority of electroactive sites on Ti/TiO_2 appear as single peaks in SECM images. The electroactive sites appear to be randomly positioned with an average spacing between sites of ca. 800 μm. As shown below, this distance is nearly 2 orders of magnitude larger than the dimensions of an individual site. Thus, in general, vast areas of the substrate are covered by a passivating oxide film on which no redox activity is visible in the SECM images.

III. Quantitative Measurement of Current Density. In this section, we describe a method for determining the rate of Br^- oxidation at individual redox-active sites on the Ti/TiO_2 surface. We assume that each site has a circular disk shape. The radially divergent transport of molecules away from microscopic sites allows sites of arbitrary shape (within reason) to be approximated as being circular without introducing significant error into the analysis.

The current at one of the microscopic sites may be expressed in terms of the surface concentration of the electrogenerated

product, C_s, and the radius of the site, a, as shown in eq 2.

$$i_{site} = 4nFDC_s a \tag{2}$$

Equation 2 is identical in form to eq 1 except that it is written in terms of the surface concentration and diffusivity of the electrogenerated product. For the reaction being considered here, C_s and D are the surface concentration and diffusivity, respectively, of electrogenerated Br_2.

Evaluation of i_{site} requires knowledge of C_s and a, neither of which is known a priori. We measure these two quantities using a procedure similar to that recently developed by Bath et al. for molecular transport from pores.[7] Briefly, for diffusion from a disk-shaped electrode, the resulting concentration profile in the solution surrounding the disk is given by[18]

$$C(r,z) = \frac{2C_s}{\pi}\tan^{-1}\frac{2a^{1/2}}{((r^2+z^2-a^2)+((r^2+z^2-a^2)^2+4z^2a^2)^{1/2})^{1/2}} \tag{3}$$

where r and z are the radial and axial coordinates, respectively, of the cylindrical coordinate system. As before, C_s is the concentration at the surface of the disk, and $C(r,z)$ is concentration of the product species at a position (r,z) in solution, measured from the center of the disk. Setting $r = 0$ yields the concentration profile of the electrogenerated product (i.e., Br_2) along the imaginary centerline axis extending into the solution, eq 4. As expected, the concentration profile, $C(r = 0,z)$, is

$$C(r = 0,z) = \frac{2C_s}{\pi}\tan^{-1}\left(\frac{a}{z}\right) \tag{4}$$

described by the same two parameters (C_s and a) that determine i_{site}. However, $C(r = 0,z)$ can be readily determined by measuring the current at the SECM tip as a function of z (equal to d, the experimental distance between the tip and substrate). Once the experimental profile, $C(r = 0,z)$, is established, eq 4 is then fit to the data using a least-squares analysis to obtain the best estimates of C_s and a. These values are then substituted into eq 2 to obtain the current at the microscopic site, i_{site}.

The preceding analysis is only approximate due to interaction between the tip and substrate, i.e., the concentration profile around the electroactive site is altered by detection at the tip. To circumvent this problem, we have developed empirical working curves based on experiments using Pt and Au microelectrodes which allow correction of the measured values of C_s and a for any possible tip interactions (vide infra).

C_s and a at Pt and Au microelectrodes of known radii were measured using either the oxidation of $Fe(CN)_6^{4-}$ or Br^- as the redox reaction. Figure 6a shows a SECM image obtained above a 12.5-μm-radius Pt disk electrode during the steady-state oxidation of $Fe(CN)_6^{4-}$. The SECM image shows the concentration profile of the electrogenerated product $Fe(CN)_6^{3-}$ in the $x-z$ plane, i.e., the plane oriented parallel to the centerline axis of the electrode (note: SECM images generally display information in a $x-y$ plane; the image in Figure 6a shows the concentration in a plane orthogonal to the $x-y$ plane). The gray scale image clearly demonstrates that $Fe(CN)_6^{3-}$ diffuses in a radial pattern away from the disk-shaped surface. Similar experiments were performed using both smaller (6-μm-radius) and larger (25-μm-radius) microdisks. The concentration profiles along the centerline axis (shown in Figure 6a as the vertical line above the electrode) were extracted from these data sets and used with curve fitting routines to extract C_s and a.

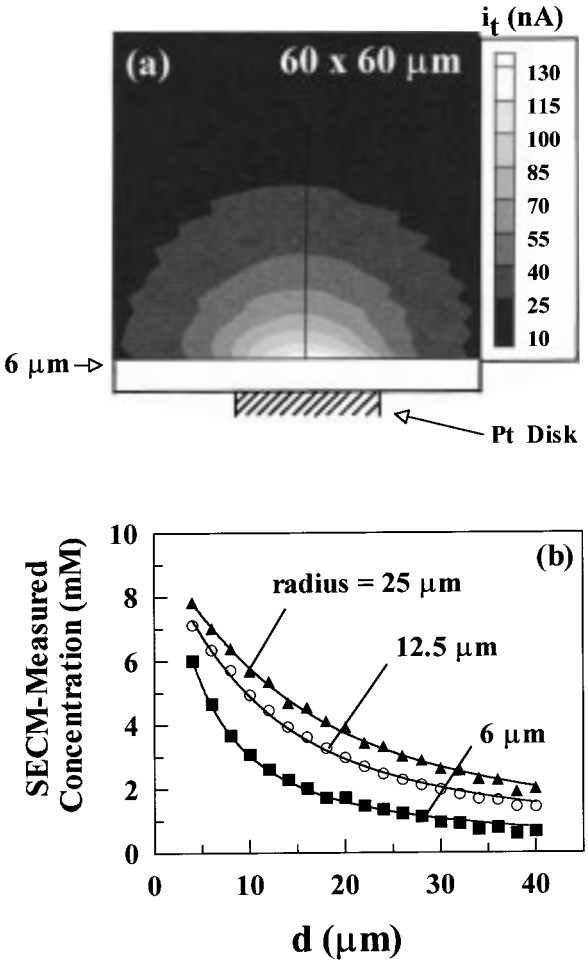

Figure 6. (a) SECM image of a 12.5-μm-radius Pt disk in a 0.1 M NaCl solution containing 10 mM $K_4Fe(CN)_6$. The image depicts the concentration distribution of electrogenerated $Fe(CN)_6^{3-}$ in the $x-z$ plane that passes through the center of the electrode. The electrode cross section and position (to scale) are represented by the shaded box drawn below the image. Data were collected beginning at a distance, d, of 6 μm above the disk surface (i.e., the rectangular white box below the image corresponds to a region of space where data were not collected). Images were obtained with $E_s = 0.6$ V and $E_t = 0.0$ V, corresponding to the oxidation of $Fe(CN)_6^{4-}$ at Ti/TiO_2 and the reduction of $Fe(CN)_6^{3-}$ at the SECM tip, respectively. (b) Concentration profiles along the z-axis, measured in solution directly above the center of the microdisk electrode (i.e., along the vertical line drawn in part (a)). Data were obtained at 12.5- and 25-μm-radius Pt disks and a 6-μm-radius Au disk electrode. The solid lines correspond to the best fits of eq 4 to the data. The surface concentration of the electrogenerated product ($Fe(CN)_6^{3-}$), C_s, and the active-site radius, a, are the two adjustable parameters used to fit the lines to the data.

The experimental profiles and fits for the three different electrodes are shown in Figure 6b.

Values of C_s and a extracted from the above SECM measurements are plotted in Figure 7 versus their expected values. Assuming the diffusivities of reactant and product are equal, the surface concentration of the electrogenerated product, C_s, is expected to be equal to the bulk concentration of the reactant, after correcting for the reaction stoichiometry. That is, oxidation of $Fe(CN)_6^{4-}$ (i.e., $Fe(CN)_6^{4-} \rightarrow Fe(CN)_6^{3-} + e^-$) in a solution containing 10 mM $Fe(CN)_6^{4-}$ is expected to yield $C_s = 10$ mM for $Fe(CN)_6^{3-}$. However, oxidation of Br^- (i.e., $2Br^- \rightarrow Br_2 + 2e^-$) results in a value of C_s for Br_2 ($\sim$25 mM) that is equal to half of the bulk concentration of Br^- (50 mM).

Figure 7a demonstrates that the SECM-measured values of C_s correspond very well with the expected values. The slope

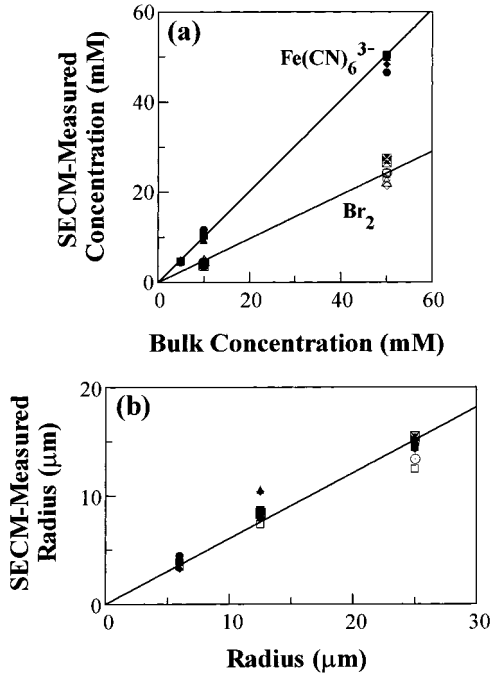

Figure 7. (a) A plot of the SECM-measured surface concentration, C_s, versus the bulk concentration of redox species. The slopes of the lines are 1.0 for $Fe(CN)_6^{3-}$ and 0.5 for Br_2. (b) A plot of the SECM-measured microdisk radii versus true radii. The slope of the line is 0.61. Experimental conditions are given in Figure 6.

TABLE 1: Estimate of Error in SECM Measurements of Surface Concentration and Radius

expt[a]	C_s (mM)[b]	a (μm)[c]
1	28.0	12.0
2	24.8	12.7
3	23.9	11.8
4	27.9	12.4
ave	26.2 ± 1.8 mM[d]	12.2 ± 0.4 μm[d]

[a] The 12.5-μm-radius Pt electrode was polished between experiments. [b] The expected value for C_s is ca. 25 mM, on the basis of a bulk KBr concentration of 50 mM, the electrode reaction, $2Br^- \rightleftharpoons Br_2 + 2e^-$, and the assumption of equal diffusivities for Br^- and Br_2. [c] The electrode radius was measured to be 12.5 ± 0.2 μm from conventional steady-state voltammetric measurements in $K_4Fe(CN)_6$ solutions. [d] One standard deviation.

of the line through the data obtained in $K_4Fe(CN)_6$ solutions is 1.0, as expected from a one-electron transfer process. Likewise, the slope of the line for data obtained for Br^- oxidation is ~0.5, as expected from a two-electron transfer process. On the other hand, poorer agreement is obtained between SECM-measured radii and the true values of the radii, Figure 7b. However, a linear fit through the data can be used to established an empirical relationship between the SECM-measured radii and the true radii. The slope of the line through the data is 0.61. Figures 7a and 7b are used in the following sections to empirically correct for nonideal tip interactions.

Table 1 shows data from four experimental trials in which C_s and a were measured for a 12.5-μm-radius Pt microdisk in a 50 mM Br^- solution. The Pt microdisk was removed from the solution and polished between each trial to determine the error associated with polishing the substrate and repositioning of the SECM tip. Using the empirical curves in Figure 7, the SECM-measured values of 26.2 ± 1.8 mM and 12.2 ± 0.4 μm were obtained for C_s and a, respectively, in good agreement with the expected values. The relative indeterminate errors in C_s (~7%) and a (3%) are primarily due to the uncertainty in d.

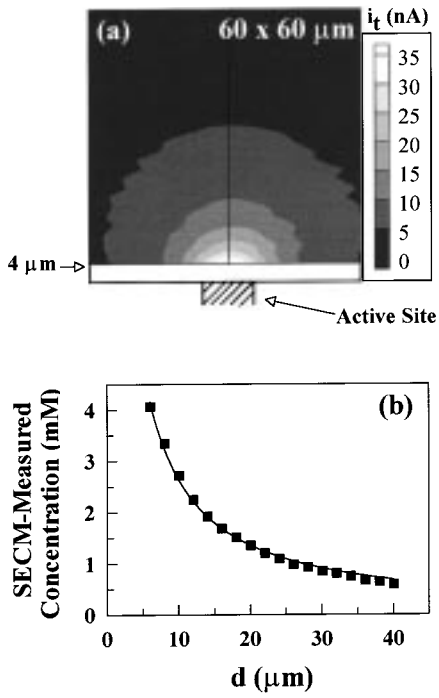

Figure 8. (a) SECM $x-z$ image of an electroactive site at Ti/TiO_2 (E_s = 1.5 V, E_t = 0.0 V) in a solution containing 50 mM KBr and 10 mM H_2SO_4. The concentration distribution corresponds to Br_2 generated at the active site and detected at the SECM tip. The active site (drawn to scale) is represented by the shaded box drawn below the image. Data were collected beginning at a distance, d, of 4 μm above the disk surface (i.e., the rectangular white box below the image corresponds to a region of space where data were not collected). (b) Concentration profile along the z-axis, measured in the direction above the center of the active site. The solid line corresponds to the best fit of eq 4 to the data, using $C_s = 1.28 \times 10^{-2}$ M and a = 5.6 μm.

IV. SECM Analysis of the Current Density at Individual Sites on Ti/TiO_2. The above analysis can be employed to measure C_s and a associated with a microscopic redox site on Ti/TiO_2. Values of C_s and a are then substituted into eq 2 to obtain the absolute current at that individual site, i_{site}.

Figure 8 shows the SECM $x-z$ image and C(r = 0,z) profile at a typical active site on Ti/TiO_2 in a solution containing 50 mM KBr and 10 mM H_2SO_4 (E_s = 1.5 V and E_t = 0.0 V). The $x-z$ image displays nearly hemispherical isocurrent contours, consistent with molecular transport of Br_2 from a disk-shaped site. Equation 4 was fitted to the C(r = 0,z) profile, Figure 8b, to obtain estimates of C_s and a, using the empirical correlation in Figure 7 to correct for nonideal tip interactions, as described above. The curve fitting analysis yields C_s = 12.8 mM and a = 5.6 μm. Inserting these values into eq 2 yields i_{site} = 135 nA. The fact that C_s is appreciably less than 25 mM indicates that oxidation of Br^- at this site occurs at a rate that is less than the mass transport value. This result suggests that the rate of Br^- oxidation is controlled by heterogeneous electron-transfer kinetics.

V. SECM Analysis of the Current Distribution. Quantitative SECM analyses of the kinetics of *every* electroactive site on three different Ti/TiO_2 electrodes was performed. The complete data set for one electrode is presented in Table 2. For this electrode, 12 redox-active sites were identified in large-area SECM images, and the corresponding values of a and C_s were measured for each, as described in the preceding section. (The electrogeneration of Br_2 at one site was too small for quantitative analysis; thus, data for only 11 sites are presented in Table 2.) The current and current density corresponding to

TABLE 2: SECM Analysis of Electroactive Sites at a Ti/TiO_2 Electrode[a]

site	a (μm)[b]	C_s (mM)[b]	i_{site} (nA)[c]	$i_{site}/\pi a^2$ (mA/cm^2)
1	17.7	3.3	110	1.1
2	16.4	0.9	27.7	3.3
3	4.5	10.3	86.2	140
4	17.7	0.6	19.9	2.0
5	13.1	0.9	22.0	4.1
6	7.3	1.2	16.4	9.9
7	7.9	16.7	249	130
8	6.0	3.8	42.4	38
9	25.5	0.3	14.3	0.80
10	9.4	1.6	28.3	10
11	28.6	0.3	16.1	0.60
			$\Sigma i_{site} = 631$ nA[d]	

[a] Measurements were made in a 10 mM H_2SO_4 solution containing 50 mM KBr. Twelve active sites were detected at this electrode; the flux of Br_2 from one site was negligibly small, preventing the analysis for a and C_s. However, the current (i_{site}) at this site was estimated to be less that 1 nA. [b] Determined by fitting eq 4 to experimental $C(z)$ vs z profiles. [c] Computed using eq 2. [d] The total steady-state current (i_{tot}) at this Ti/TiO_2 electrode was 920 nA. The fraction of current carried by the electroactive sites is $(\Sigma i_{site}/i_{tot}) \times 100 = 69\%$.

TABLE 3: Percentage of Total Electrode Current and Area Associated with Microscopic Redox-Active Sites

electrode no.	% current[a]	% area[b]
1	69	0.10
2	63	0.01
3	70	0.03

[a] Current at all redox-active sites, Σi_{site}, divided by the total current, i_{tot}, $\times$ 100. [b] Area of all redox-active sites, Σi_{site}, divided by the geometrical electrode area (0.079 cm^2) $\times$ 100.

Br^- oxidation at each site were computed using eq 2. The results are tabulated in Table 2.

The SECM analyses provide the following quantitative characteristics of the Ti/TiO_2 electrode. There are eleven active sites on the surface, having radii ranging from 4.5 to 28.6 μm. The surface concentration of Br_2 at each site is less than that expected if the reaction were mass-transport limited ($C_s \approx 25$ mM for a mass-transfer-limited reaction, see section III). However, C_s ranges from 0.3 (site no. 9) to 16.7 mM (site no. 7), indicating a wide range of electron-transfer rates at individual redox sites. The larger values of C_s, e.g., 16.7 mM, *approach* the value expected for the mass-transport-controlled reaction, indicating that the oxidation of Br^- at some sites is relatively facile. An apparent correlation between kinetic rates and the dimensions of the redox-active sites is discussed below.

The total current associated with microscopic sites is obtained by summing the current at each site, Σi_{site}. From the data in Table 2, $\Sigma i_{site} = 631$ nA. This current is equal to 69% of the total steady-state current, $i_{tot} = 920$ nA, at this Ti/TiO_2 electrode, i.e., 69% of the total current passes through the microscopic electroactive sites. From the measured values of a, the combined area of the sites on this electrode is 7.9×10^{-5} cm^2, representing only 0.10% of the total geometric area of the electrode.

It is apparent from this analyses that the electrochemical current at the Ti/TiO_2 surface is highly localized. Current densities greater than 0.1 A/cm^2 are observed at the more active sites, Table 2. For comparison, the current density computed solely on the basis of the geometric area of the electrode is 1.1×10^{-5} A/cm^2, 4 orders of magnitude smaller than the localized current density. Table 3 summarizes values of the fraction of current carried by the redox-active sites and their fractional surface coverage. For the three electrodes analyzed in detail, the fraction of current carried by the sites is relatively constant, ranging from 63 to 70%. The fractional area occupied by the sites shows a slightly larger variation, ranging from 0.01 to 0.1%. The data suggest that the microscopic current distribution is quantitatively similar on different Ti/TiO_2 electrodes.

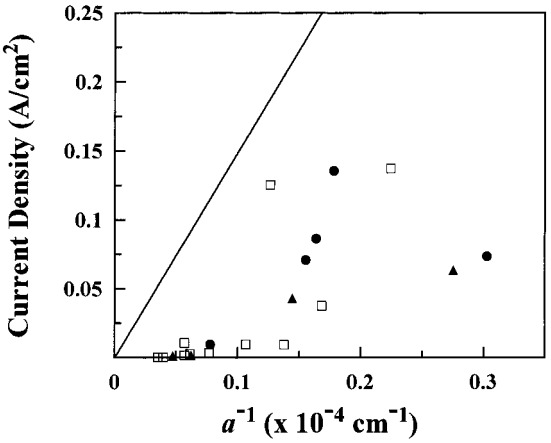

Figure 9. A plot of the current densities at active sites on Ti/TiO_2 versus the inverse of the site radii, a^{-1}. The results were obtained in a solution containing 50 mM KBr and 10 mM H_2SO_4. The solid line represents the expected dependence for the mass-transport-limited oxidation of Br^- at the sites. The finding that the data points fall below this line indicates that the oxidation of Br^- at the electroactive sites is controlled, in part, by the rate of electron transfer.

The SECM analyses indicate that ~65% of the total current passes through microscopic electroactive sites. The remainder of the current must be more evenly distributed across the remaining region of the oxide film. Whether or not this current is spread uniformly across the surface or localized to discrete sites too small to be observed by SECM is not known.

Finally, Figure 9 shows a plot of current density versus the inverse of the characteristic radius of the site, i.e., a plot of $i_{site}/\pi a^2$ vs a^{-1}. The straight line drawn in this plot represents the anticipated values of $i_{site}/\pi a^2$ if Br^- were oxidized at the mass-transport-limited rate. All experimental data for the electroactive sites fall below this line, indicating that Br^- oxidation is partially controlled by heterogeneous electron-transfer kinetics, in addition to mass transport. Interestingly, the data in Figure 9 suggest that the electron-transfer kinetic rate at smaller sites, on average, is significantly larger than that at the larger electroactive sites; i.e., the observed current density at smaller sites represents a larger *relative* fraction (30−50%) of the mass-transport-limited current than the larger sites (5%). Specifically, the current density and, thus, the kinetic rate drop precipitously at sites having radii greater than ~10 μm. We have no explanation for this behavior, other than to suggest that the chemical or physical structure of the oxide film is related to the site dimension. For instance, the results are consistent with smaller sites being covered by a thinner oxide film, allowing more rapid electron transfer between the underlying metal and the redox species. Alternatively, it may be that more than one chemically distinct type of electroactive site is present at the surface. Analysis of the electroactive sites on these Ti/TiO_2 electrodes using X-ray photoelectron spectroscopy and Auger electron spectroscopy have not revealed any differences in the oxide thickness or chemical composition at the redox-active sites.[19] Investigations are in progress to identify the chemical or structural property responsible for the electrochemical activity at these sites.[20]

Conclusion

The results of this study demonstrate that SECM is useful in quantifying the microscopic current distribution at large-area electrodes that possess a moderately complex and heterogeneous surface structure. The SECM methodology allows quantitative evaluation of the absolute current density of individual electroactive sites as well as the dimensions of the sites. Although the approach described here involves empirical correction factors to account for nonideal tip interactions, it is generally applicable to any heterogeneous surface containing an arbitrary number of randomly positioned sites, each of different size and/or displaying different electron-transfer kinetics.

SECM analysis of *every* electroactive redox site on several large-area Ti/TiO_2 electrodes has been performed, and the results used to determine the fraction of the total current flowing across the electrode/electrolyte interface that is associated with the microscopic sites. We have shown that a small number density ($\sim$180 sites/cm^2) of microscopic electroactive sites ($a_{avg} \approx 11.8$ μm), occupying a remarkably small percentage of the total exposed area (0.01 to 0.1%), can dominate the overall electrochemical behavior of the Ti/TiO_2 electrode.

Acknowledgment. This work was supported by the Office of Naval Research.

References and Notes

(1) Casillas, N.; Charlebois, S. J.; Smyrl, W. H.; White, H. S. *J. Electrochem. Soc.* **1993**, *140*, L143.

(2) Casillas, N.; Charlebois, S. J.; Smyrl, W. H.; White, H. S. *J. Electrochem. Soc.* **1994**, *141*, 636.

(3) Basame, S. B.; White, H. S. *J. Phys. Chem.* **1995**, *99*, 16430.

(4) Garfias-Mesias, L. F.; Alodan, M.; James, P. I.; Smyrl, W. H. *J. Electrochem. Soc.* **1998**, *145*, 2005.

(5) (a) Engstrom, R. C.; Weber, M.; Wunder, D. J.; Burgess, R.; Winquist, S. *Anal. Chem.* **1986**, *58*, 844. (b) Engstrom, R. C.; Meaney, T.; Tople, R.; Wightman, R. M. *Anal. Chem.* **1987**, *59*, 2005. Engstrom R. C. *Anal. Chem.* **1984**, *56*, 890.

(6) (a) Bard, A. J.; Fan, F.-R. F.; Kwak, J.; Lev, O. *Anal. Chem.* **1989**, *61*, 132. (b) Bard, A. J.; Fan, F.-R. F.; Mirkin, M. V. In *Electroanalytical Chemistry*; Bard, A. J., Ed.; Marcel Dekker: New York, 1994; Vol. 18, p 243.

(7) Morrison, S. R. *Electrochemistry at Semiconductor and Oxidized Metal Electrodes*; Plenum Press: New York, 1980.

(8) Horrocks, B. R.; Mirkin, M. V.; Bard, A. J. *J. Phys. Chem.* **1994**, *98*, 9114.

(9) Bard, A. J.; Mirkin, M. V.; Unwin, P. R.; Wipf, D. O. *J. Phys. Chem.* **1992**, *96*, 1861.

(10) Bath, B. D.; White, H. S.; Scott, E. R. *Anal. Chem.* **1998**, *70*, 1047.

(11) Zhou, F.; Unwin, P. R.; Bard, A. J. *J. Phys. Chem.* **1992**, *96*, 4917.

(12) Scott, E. R.; White, H. S.; Phipps, J. B. *Anal. Chem*. **1993**, *65*, 1537.

(13) Scott, E. R.; Laplaza, A. I.; White, H. S.; Phipps, J. B. *J. Pharm. Res.* **1993**, *10*, 1699.

(14) Potje-Kamloth, K.; Janata, J.; Josowicz, M. *Ber. Bursen-Ges. Phys. Chem.* **1989**, *93*, 1480.

(15) Ohtsuka, T.; Masuda, M.; Sato, N. *J. Electrochem. Soc*. **1985**, *132*, 787.

(16) Kwak, J.; Bard, A. J. *Anal. Chem.* **1989**, *61*, 1221.

(17) Wipf, D. O.; Bard, A. J. *J. Electrochem. Soc*. **1991**, *138*, 469.

(18) Saito, Y. *Rev. Polarogr*. **1968**, *15*, 177.

(19) Basame, S.; White, H. S., University of Utah, 1998, unpublished results.

(20) Garfias-Mesias et al. (ref 4) have reported localized redox activity at polycrystalline Ti disks that is associated with large ($\sim$5 μm diameter) impurity inclusions of Si and Al. Inclusions have not been observed on the surface of Ti foils used in the present study.